Chinese Chemical Letters 33 (2022) 2147–2150

Contents lists available at ScienceDirect

Chinese Chemical Letters

journal homepage: www.elsevier.com/locate/cclet

Azulenoisoindigo: A building block for π-functional materials with reversible redox behavior and proton responsiveness

Bin Hou[a], Jing Li[a], Xiaodi Yang[b], Jianwei Zhang[b], Hanshen Xin[a], Congwu Ge[a], Xike Gao[a,*]

[a] Key Laboratory of Synthetic and Self-Assembly Chemistry for Organic Functional Molecules, Shanghai Institute of Organic Chemistry, University of Chinese Academy of Sciences, Chinese Academy of Sciences, Shanghai 200032, China
[b] Experiment Center for Science and Technology, Shanghai University of Traditional Chinese Medicine, Shanghai 201203, China

ARTICLE INFO

Article history:
Received 26 July 2021
Revised 11 August 2021
Accepted 18 August 2021
Available online 21 August 2021

Keywords:
Azulene
Nonbenzenoid aromatic hydrocarbons
Isoindigo
π-Functional materials
Proton responsiveness

ABSTRACT

Azulene, one of representative nonbenzenoid aromatic hydrocarbons, exhibits unique molecular structure and distinctive physical and chemical properties. Herein, azulenoisoindigo (**AzII**), an azulene-based isoindigo analogue, is designed and synthesized, which has a twisted molecular backbone and *R*/*S*-isomers in single crystals. Interestingly, **AzII** shows the characteristics of both isoindigo and azulene, such as reversible redox behavior and reversible proton responsiveness. UV-vis-NIR, ^{1}H NMR and electron paramagnetic resonance (EPR) measurements were carried out to get insights into the possible mechanism of the proton-responsive property of **AzII**. The results demonstrated that only one azulenyl moiety of molecule of **AzII** was protonated and deprotonated, and the protonated **AzII** can be further oxidized to form azulenium cation radicals.

Azulene, a typical bicyclic nonbenzenoid aromatic system, can be regarded as the fusion of an electron-rich five-membered ring and an electron-deficient seven-membered ring (Fig. 1a). This non-alternant chemical structure distinguishes azulene from the isomeric naphthalene, which endows azulene with a bright blue color and a large dipole moment of 1.08 D [1]. In addition, the highest occupied molecular orbital (HOMO) and lowest unoccupied molecular orbital (LUMO) of azulene are different from those of naphthalene, showing a non-mirror-related electron density distribution [2]. This distinctive frontier orbital characteristics enable azulene with a small energy gap. Thanks to these unique structural and electronic configurations, azulene derivatives have been studied in functional organic materials [3–7] including sensory materials [8,9], Near IR (NIR) materials [10,11], organic field-effect transistors (OFETs) [12,13] and solar cells [14–16]. In recent years, more and more attention has been paid to the azulene derivatives for their applications in responsive materials [17–21]. To further explore new stimuli-responsive π-functional materials, it is imperative to develop new synthetic strategies for constructing novel azulene-based materials with proton responsiveness.

Isoindigo was identified as one of the most extensively studied moieties in antiproliferative agents [22,23] and optoelectronic materials [24–26]. It has two five-membered lactam rings con-

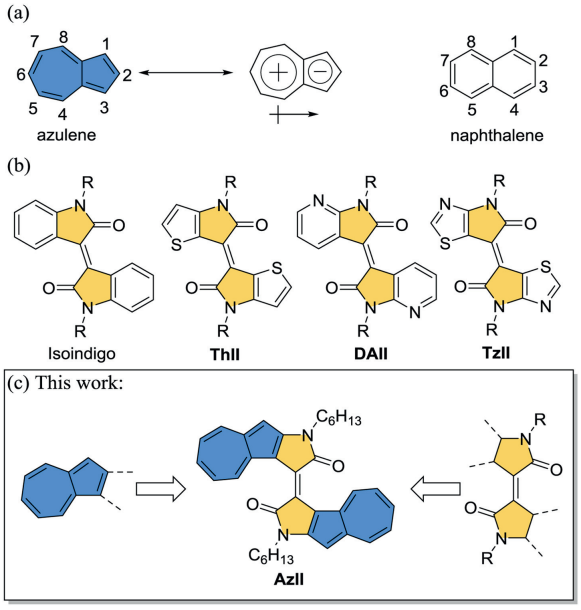

Fig. 1. Molecular structures of (a) azulene and naphthalene with atom number, (b) representative isoindigo analogues and (c) **AzII.**

* Corresponding author.
E-mail address: gaoxk@mail.sioc.ac.cn (X. Gao).

https://doi.org/10.1016/j.cclet.2021.08.079
1001-8417/

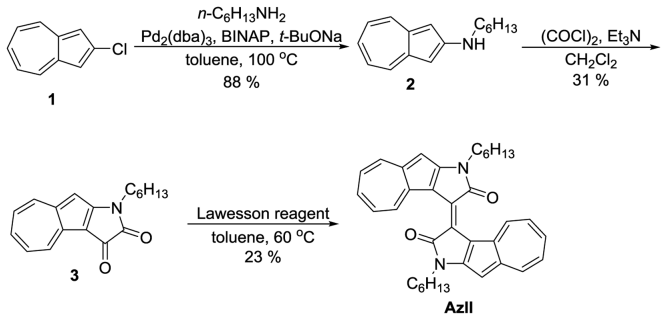

Scheme 1. Synthetic route of **AzII.**

nected with an exocyclic double bond at the 3,3'-positions and each lactam ring is fused with a benzene ring to form a conjugated structure. Since Reynolds and coworkers [27] first investigated two isoindigo-based molecules in organic solar cells (OSCs) in 2010, isoindigo was soon widely applied as a building block to construct π-functional materials [28,29]. Moreover, to explore the optoelectronic property and performance relationships of isoindigo analogues, some strategies have been developed to optimize the molecular structures [26]. Among them, one strategy is replacing the terminal phenyl rings with other aromatic rings. For example, the benzene rings were replaced by thiophene rings, pyridine rings and thiazole rings to form new isoindigo analogues, thienoisoindigo (**ThII**) [30], diazaisoindigo (**DAII**) [31–33] and thiazoloisoindigo (**TzII**) [34,35], respectively (Fig. 1b). Through the molecular structure modification, the new isoindigo analogues perform even better optoelectronic properties than those of the intrinsic isoindigo.

In recent years, our group has devoted to the study of azulene-based π-functional materials [36–40]. Herein we designed and synthesized a new isoindigo analogue, azulenoisoindigo (**AzII**), which combines the merits of azulene and isoindigo. As shown in Fig. 1c, the two lactam rings of **AzII** are fused with azulene at its 1,2-positions. The structural features and optoelectronic properties of **AzII** were explored by experimental measurements and theoretical calculations. It is worth noting that **AzII** possesses proton-responsive behavior and would be a promising material used for sensors and other electronic devices.

The synthetic strategy of azulene-based isoindigo **AzII** is shown in Scheme 1. 2-Chloroazulene (**1**) was prepared from commercially available tropolone according to the reported literature [41]. Then compound **1** underwent Buchwald-Hartwig cross coupling reaction to afford *N*-hexylazulen-2-amine (**2**) in 88% yield. By reference to the synthesis of thienoisoindigo [42] with consideration of the high electrophilic aromatic substitution reactivity of 1-position in azulene, Friedel-Crafts acylation and amidation reaction of compound **2** with oxalyl chloride were performed with triethylamine in dichloromethane affording the azulenoisatin **3** in 31% yield, which is similar to Ito's work [43]; The self-coupling reaction of azulenoisatin **3** using Lawesson reagent gave the targeted compound **AzII** in 23% yield. **AzII** showed good solubility in common organic solvents, such as CH_2Cl_2, $CHCl_3$, toluene and THF. The chemical structure of **AzII** was fully characterized with ^1H and ^{13}C NMR spectroscopy, high-resolution mass spectrometry, FT-IR spectrometry, elemental analysis, as well as single crystal analysis. The decomposition temperature of **AzII** was 302 °C defined as the 5% weight loss by a thermal gravimetric analysis (TGA), demonstrating the good thermal stability of **AzII**.

Single crystals of **AzII** grown by a slow diffusion method with dichloromethane and methanol solvents were characterized by single-crystal X-ray analysis. The single crystal analysis shows that **AzII** has an obvious twisted molecular backbone (Fig. 2). The dihe-

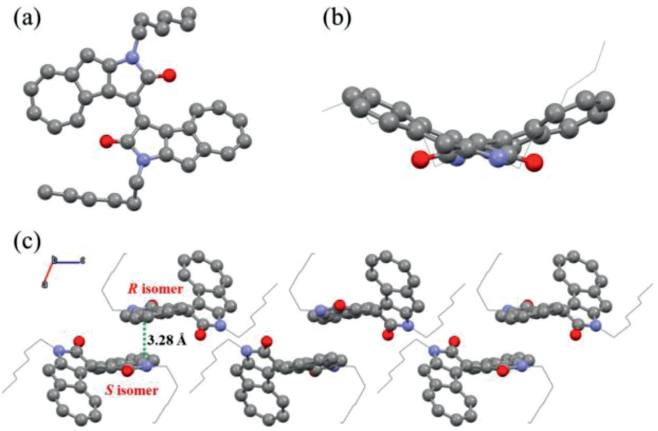

Fig. 2. Crystal structure of **AzII**: (a) top view, (b) side view and (c) molecular packing.

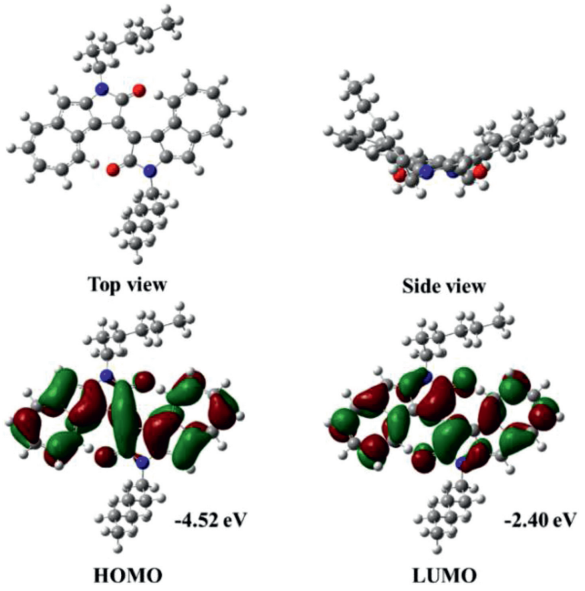

Fig. 3. Optimized molecular structure, frontier molecular orbitals and energy levels of **AzII** obtained by DFT calculations.

dral angle of the two azulenyl moieties of **AzII** is 47.80°, which is larger than those of the previously described isoindigo analogues [44,45]. It is noteworthy that there are *R*/*S* isomers in the crystal, which is probably due to the intense steric hindrance between the O atoms of lactam groups and the neighbouring H atoms at 4-position of azulenyl units. Attempts to separate the isomers by chiral HPLC failed, maybe due to the inversion of configuration of **AzII** at room temperature. The *R*/*S* isomers of **AzII** form a dimer through π-π stacking, and the interplanar distance is about 3.29 Å between the mean planes of two azulene-fused rings and the short intermolecular atom-atom contacts are among 3.36–3.37 Å between the two molecules in the dimer.

To gain an insight into the molecular geometric structure and electronic properties of **AzII**, density functional theory (DFT) calculations were carried out at the B3LYP/6–31G(d,p) level using the Gaussian 16 Program. As depicted in Fig. 3, the optimized molecular geometry of **AzII** is twisted, which is consistent with that in the single crystals. The electron density distributions of both HOMO and LUMO are widely delocalized and spread over the whole π-conjugated backbone. The calculated HOMO and LUMO energy levels of **AzII** are −4.52 and −2.40 eV, respectively.

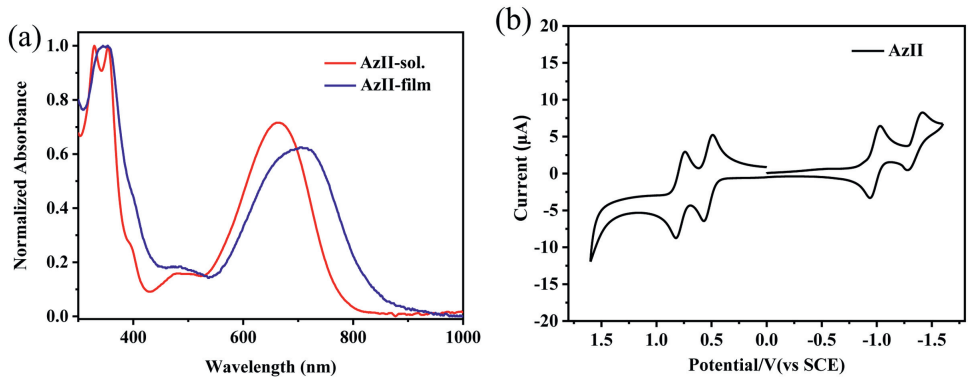

Fig. 4. (a) UV-vis-NIR absorption spectra of **AzII** in chloroform and in thin film, (b) cyclic voltammograms of **AzII** in dichloromethane (0.1 mol/L Bu_4NPF_6 as supporting electrolyte, SCE as reference electrode, scan rate of 100 mV/s).

The UV-vis-NIR absorption spectra and cyclic voltammetry (CV) of **AzII** were measured, and the related data are listed in Table S1. The UV-vis-NIR spectra of **AzII** in chloroform solution and in thin film are shown in Fig. 4a. **AzII** exhibits the broad absorption bands in the visible region with the end peak maxima at 664 nm (ε = 25,500 L mol^{-1} cm^{-1}). The spectra of **AzII** in the thin film is red shifted with an end peak at 705 nm, demonstrating the increased intramolecular conjugation and intermolecular π-π stacking in the thin film. The optical energy gap of **AzII** is calculated to be 1.60 eV from the onset of the end absorption in solution. The spectra of **AzII** are similar to those of other isoindigo analogues [44], indicating that the spectral features of **AzII** was dominated by parent isoindigo structure.

The electrochemical properties of **AzII** were investigated by CV in dichloromethane solution using 0.1 mol/L Bu_4NPF_6 as the supporting electrolyte. As shown in Fig. 4b, **AzII** presents two reversible reduction waves with the first and second half-wave potentials ($\varphi_{red}{}^{1/2}$ *vs.* SCE) at −0.98 and −1.35 V, respectively. In the positive potential region, there are also two reversible oxidation processes with the first and second half-wave potentials ($\varphi_{ox}{}^{1/2}$) *vs.* SCE of 0.53 and 0.78 V, respectively. The HOMO and LUMO energy levels of **AzII** estimated by CV (energy level of ferrocene was assumed to be −4.80 eV *versus* vacuum [46]) are −4.89 and −3.38 eV, respectively. The resulting band gap ($E_g{}^{CV}$) is 1.51 eV, which is consistent with the optical bandgap (1.60 eV) with a deviation of 0.09 eV.

Conjugated polymers and small molecules containing azulene moieties are known to be sensitive to strong organic acids such as trifluoroacetic acid (TFA) owing to the protonation of 1- or 3-position of the azulene unit [17–21]. To test the proton-responsive properties of **AzII**, TFA was added to its chloroform solution (Fig. 5). The color of **AzII** solution changed obviously from sky blue to greyish green, which can be distinguished by naked eyes. The color immediately recovered after neutralization with triethylamine (TEA). To clarify the color change, the UV-vis-NIR absorption of **AzII** upon protonation with various volume ratios of TFA was studied (Fig. 5). With the increase of volume ratios of TFA, the intensity of the absorption band at 664 nm decreased gradually. Meanwhile, a new band at 818 nm with a shoulder peak at 750 nm appeared, which was attributed to the protonation of **AzII**. When the TFA concentration was over 3% (v/v), the spectra did not change any more, suggesting the protonation state of **AzII** has reached saturation. While neutralizing with TEA, the UV-vis-NIR absorption (Fig. S2 in Supporting information) recovered almost without deviation, which is consistent with the color change observed by naked eyes.

To further investigate the mechanism of the proton-responsive feature of **AzII**, ^{1}H NMR measurements of **AzII** in the neutral and protonated state were carried out. As shown in Fig. 6, ^{1}H NMR

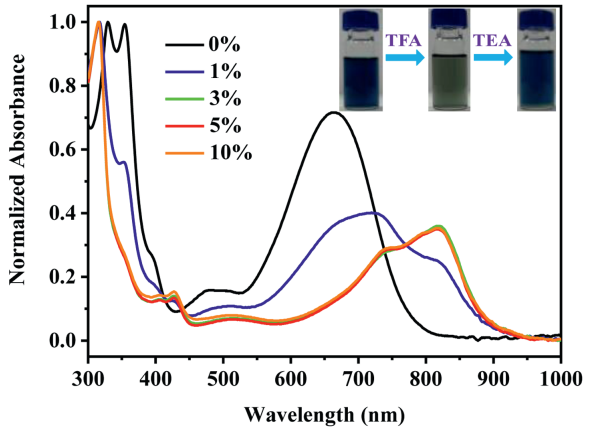

Fig. 5. Variations of UV-vis-NIR absorption spectra of **AzII** upon the protonation by TFA in chloroform.

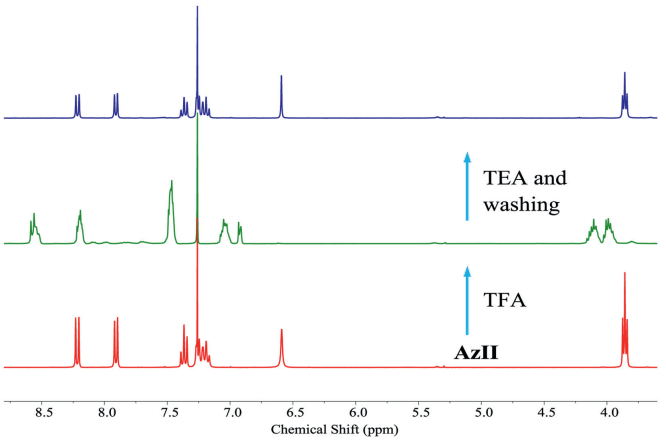

Fig. 6. ^{1}H NMR spetra of **AzII** in $CDCl_3$ by acid doping and base dedoping.

spectrum of **AzII** was broadened at aromatic regions after adding excessive TFA, whereas the split is obvious in the neutral state. Importantly, the proton signal at 3.86 ppm assigned to the CH_2 group linked with the N atom became chemical shift nonequivalence upon protonation, indicating that perhaps only one azulenyl moiety of **AzII** was protonated in the presence of excessive TFA. When the acid-doped **AzII** was neutralized with TEA and washed with water, the ^{1}H NMR spectra of **AzII** recovered well to the initial state, demonstrating the reversible proton-responsive features of **AzII**. It is known that azulene derivatives are easily oxidized after protonation to form azulenium cation radicals. Thus, a study of electron paramagnetic resonance (EPR) was conducted with the neutral and TFA-protonated **AzII** in chloroform (Fig. S3 and Table

S2 in Supporting information). Consequently, the **AzII** solution did not display any EPR signal in the neutral state, whereas a well-resolved symmetric signal with a *g*-factor value of 2.0022 and a peak-to-peak line width (ΔH_{pp}) of 7.81 G appeared after the protonation of **AzII** in solution with TFA. The quantitative EPR experiment demonstrated that only about 2.1% of TFA-protonated **AzII** converted to azulenium cation radicals, thus the protonated **AzII** still showed good NMR signals and can be neutralized by TEA. These results are consistent with previous reports of azulene-based systems [17–21]. As shown in Scheme S1, all results proposed that **AzII** possesses reversible proton responsiveness with only one azulenyl moiety of molecule protonated and the protonated **AzII** subsequently suffered from oxidation or charge transfer leading to cation radicals. This result demonstrates that **AzII** may be a potential building block for stimuli-responsive materials.

In conclusion, we have designed and synthesized an azulene-based isoindigo analogue **AzII**, which has a twisted backbone. DFT calculations, optical and electrochemical properties, as well as proton responsiveness of **AzII** were investigated. **AzII** integrates the properties of isoindigo and azulene, showing reversible redox behavior and proton responsiveness. The UV-vis-NIR, ^{1}H NMR and EPR measurements demonstrated that only one azulenyl moiety of molecule of **AzII** was protonated and deprotonated, and the protonated **AzII** can be further oxidized to form azulenium cation radicals. Our work sheds light on the significance of incorporating azulenyl moiety into classical conjugated system, and **AzII** would be a promising building block for novel π-functional materials. Further studies of **AzII**-based π-functional materials are ongoing in our lab.

Declaration of competing interest

The authors declare that they have no known competing financial interests or personal relationships that could have appeared to influence the work reported in this paper.

Acknowledgment

This research was financially supported by the National Natural Science Foundation of China (Nos. 21790362, 22075310 and 21522209), the “Strategic Priority Research Program of Chinese Academy of Sciences” (No. XDB12010100), the Science and Technology Commission of Shanghai Municipality (Nos. 19XD1424700 and 18JC1410600) and SIOC. An early preprint of this work appeared on *ChemRxiv* [47].

Supplementary materials

Supplementary material associated with this article can be found, in the online version, at doi:10.1016/j.cclet.2021.08.079.

References

[1] A.G. Anderson, B.M. Steckler, J. Am. Chem. Soc. 81 (1959) 4941–4946.
[2] J. Michl, E.W. Thulstrup, Tetrahedron 32 (1976) 205–209.
[3] J. Dong, H. Zhang, Chin. Chem. Lett. 27 (2016) 1097–1104.
[4] S. Ito, N. Morita, Eur. J. Org. Chem. (2009) 4567–4579.
[5] L. Ou, Y. Zhou, B. Wu, L. Zhu, Chin. Chem. Lett. 30 (2019) 1903–1907.
[6] H. Xin, X. Gao, ChemPlusChem 82 (2017) 945–956.
[7] H. Xin, B. Hou, X. Gao, Acc. Chem. Res. 54 (2021) 1737–1753.
[8] N. He, R.E. Gyurcsanyi, T. Lindfors, Analyst 141 (2016) 2990–2997.
[9] N. He, L. Hoefler, R. Latonen, T. Lindfors, Sens. Actuators B 207 (2015) 918–925.
[10] T. Tang, T. Lin, F. Wang, C. He, Polym. Chem. 5 (2014) 2980–2989.
[11] F. Wang, T.T. Lin, C. He, et al., J. Mater. Chem. 22 (2012) 10448–10451.
[12] Y. Yamaguchi, K. Ogawa, K. Nakayama, Y. Ohba, H. Katagiri, J. Am. Chem. Soc. 135 (2013) 19095–19098.
[13] Y. Yamaguchi, M. Takubo, K. Ogawa, et al., J. Am. Chem. Soc. 138 (2016) 11335–11343.
[14] H. Nishimura, N. Ishida, A. Shimazaki, et al., J. Am. Chem. Soc. 137 (2015) 15656–15659.
[15] T. Umeyama, Y. Watanabe, T. Miyata, H. Imahori, Chem. Lett. 44 (2015) 47–49.
[16] J. Yao, Z. Cai, Z. Liu, et al., Macromolecules 48 (2015) 2039–2047.
[17] E. Amir, R.J. Amir, L.M. Campos, C.J. Hawker, J. Am. Chem. Soc. 133 (2011) 10046–10049.
[18] E. Amir, M. Murai, R.J. Amir, et al., Chem. Sci. 5 (2014) 4483–4489.
[19] M. Murai, E. Amir, R.J. Amir, C.J. Hawker, Chem. Sci. 3 (2012) 2721–2725.
[20] M. Murai, S.Y. Ku, N.D. Treat, et al., Chem. Sci. 5 (2014) 3753–3760.
[21] K. Tsurui, M. Murai, S.Y. Ku, C.J. Hawker, M.J. Robb, Adv. Funct. Mater. 24 (2014) 7338–7347.
[22] X.K. Wee, W.K. Yeo, B. Zhang, et al., Bioorg. Med. Chem. 17 (2009) 7562–7571.
[23] Z. Xiao, Y. Wang, L. Lu, et al., Leuk. Res. 30 (2006) 54–59.
[24] X. Guo, A. Facchetti, T.J. Marks, Chem. Rev. 114 (2014) 8943–9021.
[25] T. Lei, J. Wang, J. Pei, Acc. Chem. Res. 47 (2014) 1117–1126.
[26] J. Li, J. Cao, L. Duan, H. Zhang, Asian J. Org. Chem. 7 (2018) 2147–2160.
[27] J. Mei, K.R. Graham, R. Stalder, J.R. Reynolds, Org. Lett. 12 (2010) 660–663.
[28] T. Lei, Y. Cao, Y. Fan, et al., J. Am. Chem. Soc. 133 (2011) 6099–6101.
[29] R. Stalder, J. Mei, J.R. Reynolds, Macromolecules 43 (2010) 8348–8352.
[30] R.S. Ashraf, A.J. Kronemeijer, D.I. James, H. Sirringhaus, I. McCulloch, Chem. Commun. 48 (2012) 3939–3941.
[31] G. de Miguel, L. Camacho, E.M. García-Frutos, J. Mater. Chem. C 4 (2016) 1208–1214.
[32] J. Huang, Z. Mao, Z. Chen, et al., Chem. Mater. 28 (2016) 2209–2218.
[33] Y. Lu, Y. Liu, Y. Dai, et al., Chem. Asian J. 12 (2017) 302–307.
[34] C. Li, H.-I. Un, J. Peng, et al., Chem. Eur. J. 24 (2018) 9807–9811.
[35] C. Li, H. Zhang, S. Mirie, et al., Org. Chem. Front. 5 (2018) 442–446.
[36] H. Gao, C. Ge, B. Hou, H. Xin, X. Gao, ACS Macro Lett 8 (2019) 1360–1364.
[37] B. Hou, J. Li, H. Xin, et al., Acta Chim. Sinica 78 (2021) 788–796.
[38] H. Xin, C. Ge, X. Jiao, et al., Angew. Chem. Int. Ed. 57 (2018) 1322–1326.
[39] H. Xin, C. Ge, X. Yang, et al., Chem. Sci. 7 (2016) 6701–6705.
[40] H. Xin, J. Li, R.-Q. Lu, X. Gao, T.M. Swager, J. Am. Chem. Soc. 142 (2020) 13598–13605.
[41] N. Tetsuo, S. Shuichi, M. Shingo, Bull. Chem. Soc. Jpn. 35 (1962) 1990–1998.
[42] L. Shi, Y. Guo, W. Hu, Y. Liu, Mater. Chem. Front. 1 (2017) 2423–2456.
[43] C. Kogawa, A. Fujiwara, R. Sekiguchi, et al., Tetrahedron 74 (2018) 7018–7029.
[44] T. Hasegawa, M. Ashizawa, H. Matsumoto, RSC Adv. 5 (2015) 61035–61043.
[45] Y.K. Voronina, D.B. Krivolapov, A.V. Bogdanov, V.F. Mironov, I.A. Litvinov, J. Struct. Chem. 53 (2012) 413–416.
[46] A.R. Brown, C.P. Jarrett, D.M. de Leeuw, M. Matters, Synth. Met. 88 (1997) 37–55.
[47] B. Hou, J. Li, X. Yang, et al., ChemRxiv (2021), doi:10.26434/chemrxiv.14092937.v1.